2013 European Control Conference (ECC)
July 17-19, 2013, Zürich, Switzerland.

Optimal Trajectory Planning for Standard and Hybrid Railway Vehicles with a Hydro-Mechanic Transmission

Maik Leska, Tobias Grüning, Harald Aschemann, and Andreas Rauh

Abstract— **This paper presents numerical results for the optimization of trajectories for standard diesel and hybrid railway vehicles with respect to the fuel consumption between two successive stops. First, a nonlinear model of the complete power train of a standard railway vehicle, purely driven by an internal combustion engine, is described. Based on the four different operating regimes – acceleration, cruising, coasting, and braking – fuel-optimal trajectories are computed by determining the optimal regime sequence. For this purpose, the golden ratio search method is used. Second, the presented approach is extended towards a trajectory optimization for parallel hybrid railway vehicles.**

I. Introduction

Research concerning optimal trajectory planning for trains driving between two successive stops has been a topic since the 1970s. Ichikawa [1] employed Pontryagin's maximum principle for solving a simplified optimal control problem. Shortly thereafter, Horn [2], [3] clarified by using the maximum principle that an optimal driving cycle consists of a sequence of the four regimes:

- *Accelerating* with full power,
- *Cruising* at constant speed,
- *Coasting*, and
- *Braking* with full power.

Based on these four regimes, several methods were developed in the literature that determine switching points in time and/or the speed of the cruising phase. In general, these methods can be classified into the following two groups [4]:

- Analytic solutions and
- Numeric optimization.

An analytic solution is characterized by the fact that the optimal sequence of driving regimes is determined by using a heavily simplified linear model by exploiting, e.g., Pontryagin's maximum principle, cf. [2], [3]. The system model is mainly simplified by approximating the air resistance force and by assuming that the efficiency of the propulsion system is constant for all operating points. The analytic optimization procedure leads to a minimization of the mechanical energy at the wheel but not to a minimization of the energy that is in fact provided by the propulsion system. Numeric optimization procedures typically make use of a more detailed train model and, additionally, of a discrete search space. Dynamic programming techniques are the most common methods in this field, see [5], [6]. Due to the high computational burden, dynamic programming is mainly used in combination with other methods, especially analytical ones. Further solutions like evolutionary algorithms [7] or fuzzy logic approaches [8] can be found as well in the literature.

M. Leska, H. Aschemann, and A. Rauh are with the Chair of Mechatronics, University of Rostock, Germany. {Maik.Leska, Tobias.Gruening, Harald.Aschemann, Andreas.Rauh}@uni-rostock.de, T. Grüning was with the same institute while this work was performed.

In this paper, a model-based approach to optimal trajectory planning is presented for both standard diesel and hybrid railway vehicles with a hydro-mechanic gear box. The main difficulty while dealing with hydro-mechanic transmissions is to determine the usable traction force, which strongly depends on the actual gear. The shifting points again depend on the rotational speed and the load at the gear box input. To consider these dependencies, the trajectory planning algorithm is integrated into the simulation structure, making the actual gear available at each point of time.

Sec. II presents an algorithm for the optimal trajectory planning of a standard diesel railway vehicle. First, the simulation structure used for all calculations is described in Sec. II-A. Second, in Sec. II-B the algorithm that is employed for the computation of optimal trajectories is given, which combines heuristic and optimization approaches. In Sec. III, the optimization procedure is extended towards trajectory optimization for hybrid railway vehicles. For that purpose, additional system components are added to the simulation structure which are only present in the hybrid train architecture. Additionally, the heuristic method for the construction of the velocity profile is adapted. A simple operating strategy from [10] is used to distribute the power demand between the internal combustion engine and the energy storage that is available in the hybrid system. Sec. IV concludes this paper and gives an outlook on future research.

II. Trajectory Planning for Standard Diesel Railway Vehicles

As the basis for trajectory optimization, a nonlinear simulation model is used. The simulated vehicle is a two-coach diesel multiple unit (DMU) VT642 with one propulsion unit per coach. Fig. 1 shows a basic block diagram of the single-coach propulsion unit. It consists of an internal combustion engine (ICE), a clutch C, the hydromechanic transmission, and the axle gear. The ICE provides the traction power to the power train and simultaneously supplies the mechanical auxiliaries. The clutch C is used to separate the ICE from the power train while the train is waiting at a stop.

A. Simulation Model

In Fig. 2, the simulation structure corresponding to the system architecture introduced in Fig. 1 is depicted. In this

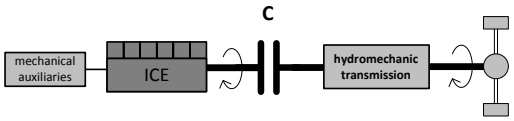

Fig. 1. Basic architecture of a standard diesel railway vehicle.

simulation, only the main effects contributing to the longitudinal dynamics of the power train are taken into account. The individual blocks represent models for the physical system components. For each component, a low-order model has been derived in [9], where either dynamic equations or static characteristic maps are implemented in Matlab/Simulink. The arrows in Fig. 2 represent the numerical evaluation order of the subcomponents and not the direction of power flow. Note, that this evaluation order is opposed to the direction of power flow, corresponding to an inverse problem. In such a

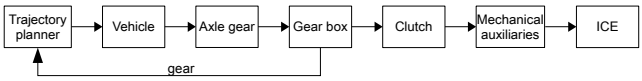

Fig. 2. Simulation structure for a standard diesel hydromechanic railway vehicle[1].

way, the inputs of the simulation approach are the velocity and altitude profiles, whereas the outputs are the load points and the fuel consumption of the ICE. The desired velocity of the DMU is calculated by the trajectory planner, which is directly included in the simulation structure according to Fig. 2. This has the advantage that the actual gear is known in the trajectory planner at each point of time. In such a way the maximum traction force can be calculated directly as a function of the gear ratio.

According to Fig. 2, the mechanical auxiliaries are supplied directly by the ICE during the whole driving cycle. The power $P_{aux,m}$ of the mechanical auxiliaries can be determined by

$$P_{aux,m} = P_{aux,c} + p_m \cdot P_{ICE} \tag{1}$$

with the constant part $P_{aux,c}$ and the load-dependent cooling term $p_m \cdot P_{ICE}$, $p_m = 0.08$.

Due to the symmetric vehicle architecture, only one propulsion system needs to be simulated. The requested overall power/torque is divided by the number of coaches (i.e., the number of propulsion systems) inside the vehicle block of Fig. 2. After completion of the simulation, the resulting fuel consumption is again multiplied by the number of coaches to obtain the overall value for the whole train.

B. Optimization Algorithm

Velocity profiles on a train track are mainly constrained by vehicle specifications, track resistances, speed limits, and the maximum admissible operating time. Nevertheless, the driver can follow different strategies to reach the final destination. To save fuel, nowadays, train drivers are instructed to act according to the four regimes: *accelerating* with full power, *cruising*, *coasting*, and *braking* with maximum deceleration. The energy-optimal driving cycle can be found by optimization of the switching points between those regimes [3]. For that purpose, linearized or highly simplified equations of motion are generally used in the literature. In this paper, the equations of motion contain all important nonlinearities of the power train as well as the auxiliaries. The dynamic system model is evaluated numerically with a discretization interval of 1 s. The velocity profile is determined by means of the trajectory planner block, see Fig. 2. First, the maximum traction force or braking force, respectively, is calculated as a function of the actual gear. The maximum acceleration/deceleration is bounded by $a \in [-a_{max}, a_{max}]$, $a_{max} = 0.9\ \mathrm{m/s^2}$ to maintain a good driving comfort. To consider the traction power limitation resulting from the rail-wheel contact, a constant maximum traction force at wheel is used. Second, the velocity of the train is calculated by a nonlinear model. By solving the equation of motion

$$k_1 \cdot m_{veh} \cdot a = F_{trac} - F_{res} - F_{inc} \tag{2}$$

for the acceleration a, the velocity v of the train can be calculated according to

$$v(t) = \int_0^t a(\tau)\, d\tau + v(0). \tag{3}$$

In (2), m_{veh} denotes the mass of the vehicle and k_1 is a factor that accounts for all rotating masses. The downhill slope force F_{inc} depends on both the mass of the vehicle m_{veh} and the inclination angle γ according to

$$F_{inc} = \sin(\mathrm{atan}(\gamma)) \cdot m_{veh} \cdot g\,. \tag{4}$$

The resistance force $F_{res} = F_{roll} + F_{air}$ represents the sum of the rolling resistance F_{roll}, which can be calculated by

$$F_{roll} = \cos(\mathrm{atan}(\gamma)) \cdot m_{axle} \cdot c_r\,, \tag{5}$$

and the air resistance F_{air}, given by

$$F_{air} = \frac{1}{2} \cdot A_{veh} \cdot \rho_{air} \cdot c_w \cdot v^2\,. \tag{6}$$

In (5) and (6), ρ_{air} is the density of air, A_{veh} is the front surface of the train, m_{axle} stands for the mass at the powered axle and c_r and c_w are the drag coefficients for the rolling resistance and the air resistance, respectively.

A combination of a heuristic with a numeric optimization approach is used to compute optimized velocity profiles for the train track. In a first step, the time-optimal driving cycle is calculated, which is only composed of acceleration, cruising at full speed, and braking. In a second step, the track is divided into N subsections with fixed initial and final states consisting of time, position, and speed information (t, s, v). Each subsection contains the run between two consecutive train stops. In reality, trains do not only drive with full power and maximum speed. Hence, the driving time t_k for

[1]To guarantee causality of the simulation model, the computation of the maximum traction force characteristics makes use of the gear information from the previous discretization time step.

each subsection is increased by ten percent as compared to the time-optimal profile. This allows for an additional driving regime (coasting) and different regime sequences. A summary of the possible regime sequences is given in Fig. 3.

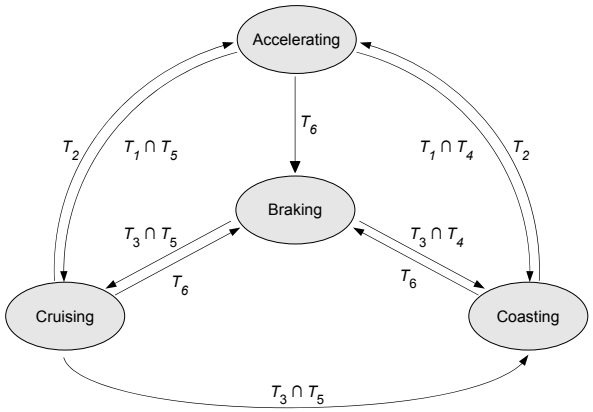

Fig. 3. Possible regime sequences.

Each subsection starts with an acceleration phase up to the desired velocity v_d or to the speed limit v_{lim}. Generally, this phase is followed by cruising and coasting phases and, finally, by a braking phase to come to a stop. A switch between two regimes occurs if one of the transitions in Fig. 3 with

- $T_1 := (v = v_d) \cup (v = v_{lim})$,
- $T_2 := (v < v_{lim}) \cap (v < v_d)$,
- $T_3 := (v = v_b) \cap (v > 0)$,
- $T_4 := (s > s_{cr})$,
- $T_5 := (s \leq s_{cr})$, and
- $T_6 := (s \geq s_b) \cap (v > v_b)$,

is activated. It is excluded that more than one transition is activated simultaneously. The parameter s_{cr} characterizes the maximum distance of the cruising mode. The braking distance s_b defines the position where the train has to start braking to come to a stop at the following station or to meet upcoming speed limits. Within the simulation structure given in Fig. 2, it is checked in each time step whether the braking distance s_b is reached. The train keeps on braking until the final braking velocity v_b is reached.

To optimize the switching points, the optimization parameter p_{va} is introduced. It specifies the desired velocity $v_d = p_{va} \cdot v_{max}$ in terms of $p_{va} \in [0,1]$ with the maximum physically possible velocity v_{max} of the train. Fig. 4 shows a typical profile generated by the trajectory planner. The final distance of the cruising phase s_{cr} is calculated numerically by a bisection method. After the train has reached the end of the cruising phase, it starts to coast. Finally, braking begins at the braking point s_b to stop at the station.

The optimal switching points between the regimes for each subsection $k = 1,2,...,N$ can be calculated by minimizing the cost function

$$J^k(p_{va}^k) = V^k(p_{va}^k). \tag{7}$$

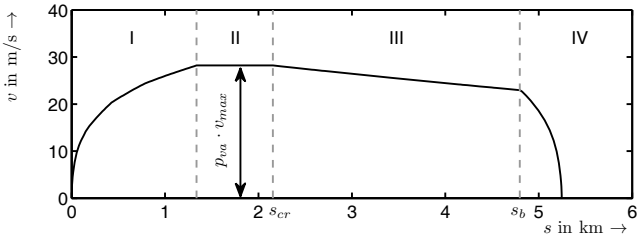

Fig. 4. Principle of the trajectory planner (I: accelerating, II: cruising, III: coasting, IV: braking).

In contrast to the approaches in [1] – [6], the fuel consumption V is minimized instead of the kinetic energy. This has the advantage that all efficiency factors of the power train components, including the ones of the ICE and the auxiliaries are considered. The fuel consumption V is calculated by an evaluation of the simulation model presented in Fig. 2.

C. Optimization Results

The optimal trajectory is calculated for the VT642, a two-coach regional DMU, running on a typical regional track. The track contains 13 stops and has the length $s_{track} = 37169$ m. The altitude profile is negligible. Due to different speed limits for the forth and back directions, the train journey is simulated and optimized in both directions. This leads to a multi-stage optimization problem with $N = 26$ subsections.

First, the time-optimal trajectory is calculated by using only the regimes *acceleration*, *cruising*, and *braking*. Fig. 5 shows the resulting complete velocity profile. In total, the train needs $t_f = 4709$ s with an overall fuel consumption of $V_{to} = 96.0$ l. The grey shadowed area shows the speed limits. On the basis of this trajectory, a time reserve of ten percent is added to the operating time for each individual subsection. The stopping times at the stations are left unchanged, since the ICE has to run at theses points to provide the power for the mechanical auxiliaries.

The cost function (7) is minimized for all subsections $k = 1,2,...,N$ (with increased operating time) by using the golden ratio search method. The resulting trajectory is depicted in Fig. 5. The overall fuel consumption for the optimized

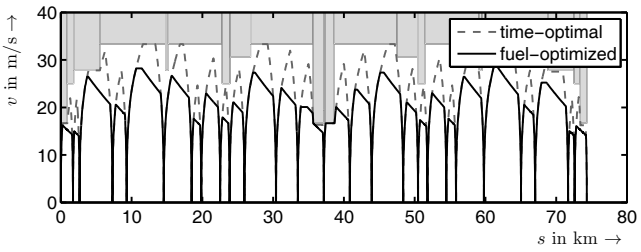

Fig. 5. Fuel-optimal trajectory for a standard diesel railway vehicle.

trajectory is $V_{opt} = 59.9$ l. The operating time including the stopping times is $t_f = 5146$ s.

In Table I, the optimization results are summarized. For a comparison, the simulation results of the time-optimal

trajectory are also presented. Hence, by an optimization of the driving cycle, fuel savings of 37.6 % could be achieved for a time reserve of 10 %. Note, that the optimization is done completely off-line, hence it is only valid for non-disturbed journeys. Such disturbances arise e.g. if one train overtakes another one, if a preceding train cannot be overtaken, or in the case of a tight sequence of trains entering a station.

TABLE I
OPTIMIZATION RESULTS FOR A STANDARD DIESEL RAILWAY VEHICLE

	s_f in m	t_f in s	V in l	Fuel savings in %
Time-optimal	74338	4709	96.0	0
Fuel-optimized	74338	5146	59.9	37.6

III. TRAJECTORY PLANNING FOR HYBRID RAILWAY VEHICLES

The power train of a basic parallel hybrid railway vehicle mainly consists of an ICE, an energy storage device, and an additional propulsion system [9]. In Fig. 6, a simplified structure of a diesel parallel hybrid railway vehicle is presented. Here, the ICE is supported by an electric motor/generator (M/G), which is directly connected to the drive shaft. The power for the electric motor is supplied by a Lithium-Ion battery. Furthermore, the battery provides the power for all electrical auxiliaries. The power transmission from the ICE

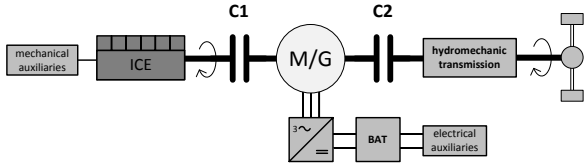

Fig. 6. Architecture of a basic diesel parallel hybrid railway vehicle.

and the M/G is achieved via a hydromechanic gear box. The clutches C1 and C2 separate either the ICE and/or the M/G from the drive shaft. By this architecture, the following six operating modes become possible:

- Mode 1: Pure ICE
- Mode 2: Pure M/G
- Mode 3: Boosting
- Mode 4: Load level increasing
- Mode 5: Coasting
- Mode 6: Recuperation

In Mode 1, the ICE provides the total power demand. Mode 2 is the pure electric mode, thus, only the electric motor is active. In Mode 3, the power boost mode, both the electric motor and the ICE operate simultaneously. In the load level increase (Mode 4), the operating point of the ICE provides more power than required for following the pre-specified duty cycle. The excess power is used for recharging the energy storage device. This mode can also be used at standstill to recharge the energy storage. In this phase, the clutch C2 is open. In Mode 5, the coasting mode, neither the electric motor nor the combustion engine are running, while the vehicle is decoupled from all engines by opening C1 and C2. Finally, in Mode 6, the recuperation mode, kinetic energy of the vehicle is recovered in deceleration phases. Opening the clutch C1 allows for decoupling of the ICE from the drive shaft. In all six operating modes, the ICE is running to supply the mechanical auxiliaries with the required power.

A. Simulation Model

The simulation model of the standard diesel railway vehicle, given in Fig. 2, is extended by the blocks for the additional components of the hybrid vehicle (M/G, current converter, energy storage, electrical auxiliaries). Fig. 7 shows the extended simulation structure for the hybrid diesel railway vehicle. Again, the individual blocks represent the models of the system components and the arrows represent the numerical evaluation order of the subcomponents and not the directions of power flow. Due to space requirements, the clutches $C1$ and $C2$ are not depicted in Fig. 7. However, they are implemented in the simulation tool. These clutches and the current converter are represented, for sake of simplicity, by constant efficiency factors. For the energy storage, a simple model of a Lithium-Ion battery is used. Its electric equivalent circuit consists of a state-of-charge-controlled voltage source in series with a constant resistance representing Ohmic losses [9]. The M/G supports the ICE during traction and charges the energy storage during braking. The M/G is modeled by a static efficiency map. For more information the reader is referred to [9], where a detailed modeling for all components is given.

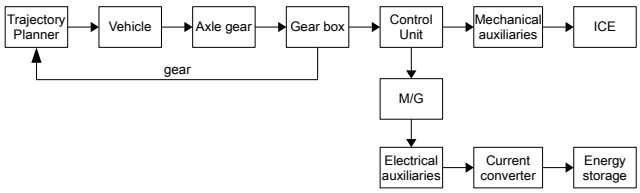

Fig. 7. Simulation structure of a diesel hydromechanic hybrid railway vehicle.

Inside the control unit, the requested power for following the duty cycle is distributed between the ICE and the M/G corresponding to the operating strategy. The inputs of the control unit are the rotational speed of the drive shaft, the requested power, the state of charge, and the maximum charging and discharging power of the Lithium-Ion battery. The outputs are the power requests for the ICE and the M/G.

The auxiliaries of the hybrid architecture are split into mechanical and electrical auxiliaries according to

$$P_{aux,m} = (1 - p_{el}) \cdot P_{aux,c} + p_m \cdot P_{ICE} \quad \text{and} \\ P_{aux,el} = p_{el} \cdot P_{aux,c}\,. \tag{8}$$

Here, $P_{aux,m}$ stands for the mechanical auxiliary power and $P_{aux,el}$ for the electrical auxiliary power. As in Sec. II, $P_{aux,c}$ denotes a constant auxiliary power, which has to be provided by the propulsion system. By means of $p_{el} \in [0,1]$, the constant power $P_{aux,c}$ is split up into a mechanical and an electrical part. As in Sec. II-A, the parameter p_m characterizes the cooling power demand of the ICE which has to be added to the mechanical auxiliaries.

The trajectory planner is again included in the simulation model. It calculates the velocity profile considering the maximum traction/braking force and the track specifications, like distance, time, and speed limits.

B. Calculation of Optimal Trajectories for Hybrid Vehicles

The main differences between a purely diesel-driven vehicle and a hybrid vehicle are the availability of an additional propulsion system and the energy storage device. Basically, the hybrid vehicle can accelerate with a higher power than the standard vehicle, if the boosting mode is used. This leads to a shorter acceleration phase, which in general yields fuel savings. However, due to the limited torque transmission ($M_{max} = 1800$ Nm) of the hydromechanic gear box, it is impossible in the current setting to supply more power than the ICE can provide without exceeding the torque limitation.

To improve the overall efficiency of the hybrid railway vehicle, it is helpful to increase the percentage of recuperated energy in braking phases by an appropriate trajectory planning. The amount of recuperated energy mainly depends on the power limitations of the system components (i.e. M/G, gear box, battery) and on the velocity profile (especially the slope of the braking phase). If the recuperable braking power is limited by some components, e.g. the maximum transmission torque of the hydro-mechanic gear box, it might be meaningful to adjust the velocity profile. This will be investigated in the following section.

First, the time-optimal trajectory for the hybrid architecture, given in Fig. 6, is calculated. Again, the regional DMU VT642 is simulated. The mass of the train is increased by 3000 kg to account for the additional components. The track topologies and the speed limits are identical to the ones in Sec. II. Fig. 8 shows the resulting trajectory. It only consists of the three regimes accelerating with full power, cruising with maximum velocity, and braking with maximum deceleration force. The purely diesel-driven train consumed $V = 97.6$ l, which is 2 % more than the standard vehicle has needed. This is caused by the increased mass of the hybrid vehicle. All in all, the train needs $t_f = 4737$ s from the starting point to the final destination.

For the calculation of optimal trajectories in hybrid operations, again ten percent time reserve is added to the operating time of the time-optimal trajectory. A boosting factor x is introduced to influence the operating strategy, which reflects the distribution of the requested power between the ICE and the M/G [10]. The boosting factor $x \in [-1,1]$ characterizes the distribution of the requested power P_{req} according to

$$P_{ICE} = (1-x) \cdot P_{req} \quad \text{and} \quad P_{M/G} = x \cdot P_{req}\,. \tag{9}$$

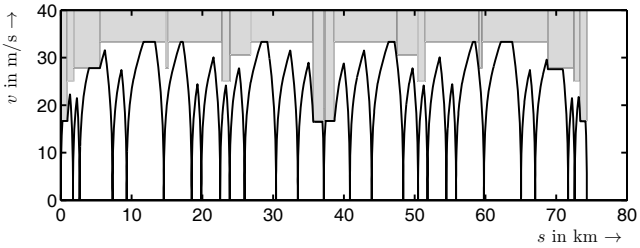

Fig. 8. Time-optimal trajectory for a hybrid railway vehicle.

Thus, $x = 0$ means a purely diesel and $x = 1$ a purely electrical drive. If $x < 0$, Mode 4 is used to recharge the battery. The state of charge (SOC) at the destination and at the starting point have to be balanced for all subsections $SOC(t_k) = SOC(t_{k-1})$ to have a fair comparison with the purely diesel-driven vehicle. Generally, $SOC(0) = SOC(t_f)$ would be enough, but for the sake of simplicity, the balanced SOC is demanded for each subsection k. The distribution of the auxiliaries is set to $p_{el} = 0.5$ which means that half of the corresponding power is consumed by the mechanical and half by the electrical auxiliaries. The operating strategy is implemented in such a way, that firstly the electrical auxiliaries will be supplied by the recuperated power and that the excess power is then used to support the ICE in traction phases. The balanced SOC is reached by adjusting the parameters $x = x^k$ for each subsection by a bisection method. The optimized trajectory is calculated by minimizing the multi-stage optimal control problem

$$J^k(p_{va}^k, x^k) = V^k(p_{va}^k, x^k)\,, \tag{10}$$

where the golden ratio search method is used. In each function evaluation, first the length of the cruising phase and the boosting factor are computed by bisection methods. Then, a simulation is performed and the cost function (10) is evaluated. This is repeated until the aborting criterion is fulfilled. The corresponding trajectory is depicted in Fig. 9.

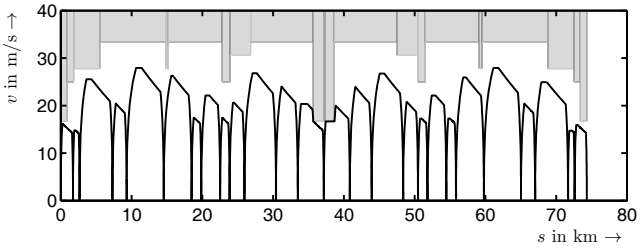

Fig. 9. Fuel-optimized trajectory for a hybrid railway vehicle.

The overall fuel consumption is $V = 48.9$ l with a driving time of $t_f = 5146$ s. This corresponds to fuel savings of 18.4 % compared to the fuel-optimal trajectory for the standard railway vehicle, see Tabs. I and II.

An analysis of the recuperated braking energy shows that only 44 % of the available braking energy at the wheel $E_{br} =$ 107 kWh is recuperated by the battery. The losses are mainly caused by the limitation of the input torque of the gear box

and the efficiency of the electrical M/G. A reduction of the braking force could lead to a better percentage of recuperated braking energy. To adjust the braking force, the parameter $q = q^k$ is introduced for each subsection. By means of q, the braking force is reduced to $F_b = q \cdot F_{b,max}$.

The physically maximum braking force $F_{b,max}$ is limited by the maximum braking power/force at the wheel, which is defined by the rail-wheel contact and the maximum deceleration. Hence, the optimal control problem can be formulated as

$$J^k(p_{va}^k, x^k, q^k) = V^k(p_{va}^k, x^k, q^k). \tag{11}$$

A cascaded optimization approach is used to minimize the cost function (11). In an inner loop, the optimal control problem (10) is solved as described above. For each parameter q^k determined by the outer loop, the inner loop is re-started and gives back the fuel consumption for the optimal trajectory. In the outer loop, the optimal parameters q^k are determined also by applying a golden ratio search method.

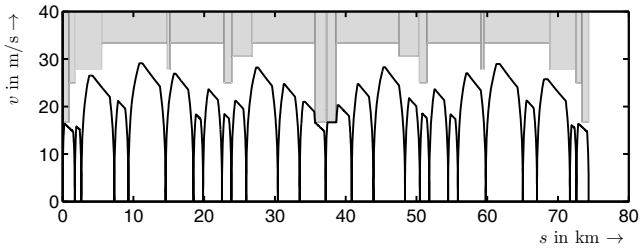

Fig. 10. Fuel-optimized trajectory for a hybrid railway vehicle.

The resulting trajectory is presented in Fig. 10. The train needs $t_f = 5146$ s for the complete driving cycle and it consumes $V = 44.5$ l. This leads to a reduction of the fuel consumption of 25.7 % as compared to the fuel-optimal diesel trajectory. The percentage of the recuperated energy is increased to 69 %. This is caused by the increased braking energy at the wheel $E_{br} = 116$ kWh, because of the higher velocity, that is necessary to drive the same distance in the same time, and the reduced power while braking causing a reduction of losses due to the torque transmission limitation of the gear box. In such a way, the input torque limitation of the gear box is inactive for most of the braking phase. Tab. II summarizes the results of the optimizations for a hybrid vehicle. In the first row, the results for the optimal trajectory by adjusting p_{va}^k and x^k are given. The train accelerates and brakes with full power. In the second row, the parameter q^k is adjusted additionally. Then, the train does not brake with maximum power and is able to recuperate more energy over the whole driving cycle. For each scenario, the overall distance, time, fuel consumption, and the fuel savings compared to the optimal trajectory for a standard vehicle are given.

TABLE II

OPTIMIZATION RESULTS FOR A HYBRID RAILWAY VEHICLE

	s_f in m	t_f in s	V in l	Fuel savings in %
Diesel	74338	5146	59.9	0.0
Hybrid 1	74338	5146	48.9	18.4
Hybrid 2	74338	5146	44.5	25.7

IV. Conclusions and Outlook on Future Research

In this paper, algorithms to calculate fuel-optimal trajectories for standard diesel and hybrid railway vehicles with a hydromechanic transmission have been presented. A trajectory planning algorithm, which combines a heuristic method to compose the speed profile (out of the four regimes: *acceleration* with full power, *cruising*, *coasting*, and *braking*) and an optimization approach to determine the switching points in the driving regime, has been developed. The trajectory planner is directly integrated into the nonlinear simulation model to get information about the actual gear at each point of time. This information is necessary to determine the maximum traction force of the power train. All speed profiles were calculated completely off-line and are only valid for non-disturbed journeys. The best optimization results for a diesel-hybrid railway vehicle, by adjusting the speed profile, show fuel savings of 25.7 % compared to a standard diesel vehicle.

In future research, alternative hybrid architectures, e.g. diesel-electric, will be investigated. Furthermore, an improved operating strategy will be used to calculate the fuel-optimal drive between two successive stations.

References

[1] K. Ichikawa, *Application of Optimization Theory for Bounded State Variable Problems to the Operation of a Train*, Bulletin of Japanese Society of Mechanical Engineering, Vol. 11, No. 47, pp. 857-865, Nov. 1968

[2] P. Horn, *Über die Anwendung des Maximumsprinzips von Pontrjagin zur Ermittlung von Algorithmen für eine energieoptimale Zugsteuerung*, (in German) Wissenschaftliche Zeitschrift der Hochschule für Verkehrs-wesen "Friedrich List", 18(4), pp. 919-943, 1971

[3] P. Horn, *Beitrag zur Lösung des Syntheseproblems der energieoptimalen Steuerung einer Zugfahrt*, Dissertation, (in German) Hochschule für Verkehrswesen "Friedrich List", Dresden, 1973

[4] Y. Wang, B. Ning, F. Cao, B. De Schutter, T.J.J. van den Boom, *A Survey on Optimal Trajectory Planning for Train Operations*, IEEE Int. Conf. on Service Operations, Logistics, and Informations (SOLI), 2011

[5] R. Franke, P. Terwiesch, M. Meyer, *An Algorithm for the Optimal Control of the Driving of Trains*, Proc. of the 39th IEEE Conf. on Decision and Control, Sydney, Australia, pp. 2123-2128, Dec. 2003

[6] R. Franke, P. Terwiesch, M. Meyer, *Optimal Control of the Driving of Trains*, at-automatisierungstechnik 50, pp. 606-613, 2002

[7] C.S. Chang, S.S. Sim, *Optimising Train Movements Through Coast Control Using Genetic Algorithms*, IEE Proc. Electric Power Applications, Vol. 144, No.1, 1997

[8] C.S. Chang, Y.H. Phoa, W. Wang, B.S. Thia, *Economy/Regularity Fuzzy-Logic Control of the DC Railway Systems Using Event-Driven Approach*, IEE Proc. Electric Power Applications Vol. 143, No.1, 1996

[9] M. Leska, T. Grüning, H. Aschemann, A. Rauh *Optimization of the Longitudinal Dynamics of Parallel Hybrid Railway Vehicles*, IEEE Multi-Conference on Systems and Control, Dubrovnik, Croatia, 2012

[10] M. Leska, R. Prabel, A. Rauh, H. Aschemann, *Simulation and Optimization of the Longitudinal Dynamics of Parallel Hybrid Railway Vehicles.*, Proc. of FORMS/FORMAT-2010, Braunschweig, Germany, Part 2, pp. 155-164, vol. 281, Springer-Verlag, 2011